Title

Cool seafloor hydrothermal springs reveal global geochemical fluxes

Authors

Wheat, C Geoffrey
Fisher, Andrew T
McManus, James
et al.

Publication Date

2017-10-01

DOI

10.1016/j.epsl.2017.07.049

Peer reviewed

Earth and Planetary Science Letters 476 (2017) 179–188

Contents lists available at ScienceDirect

Earth and Planetary Science Letters

www.elsevier.com/locate/epsl

Cool seafloor hydrothermal springs reveal global geochemical fluxes

C. Geoffrey Wheat [a,*], Andrew T. Fisher [b], James McManus [c,d], Samuel M. Hulme [e], Beth N. Orcutt [d]

[a] University of Alaska Fairbanks, PO Box 475, Moss Landing, CA 95039, United States
[b] Earth and Planetary Sciences Department, 1156 High Street, University of California, Santa Cruz, CA 95064, United States
[c] Department of Geosciences, The University of Akron, Akron, OH, 44326, United States
[d] Bigelow Laboratory for Ocean Sciences, 60 Bigelow Drive, East Boothbay, ME 04544, United States
[e] Moss Landing Marine Laboratory, Moss Landing, CA, 95039, United States

ARTICLE INFO

Article history:
Received 1 December 2016
Received in revised form 26 July 2017
Accepted 28 July 2017
Available online xxxx
Editor: D. Vance

Keywords:
hydrothermal
ridge flank
geochemical fluxes
dissolved oxygen
crustal alteration

ABSTRACT

We present geochemical data from the first samples of spring fluids from Dorado Outcrop, a basaltic edifice on 23 M.y. old seafloor of the Cocos Plate, eastern Pacific Ocean. These samples were collected from the discharge of a cool hydrothermal system (CHS) on a ridge flank, where typical reaction temperatures in the volcanic crust are low (2–20 °C) and fluid residence times are short. Ridge-flank hydrothermal systems extract 25% of Earth's lithospheric heat, with a global discharge rate equivalent to that of Earth's river discharge to the ocean; CHSs comprise a significant fraction of this global flow. Upper crustal temperatures around Dorado Outcrop are ~15 °C, the calculated residence time is <3 y, and the composition of discharging fluids is only slightly altered from bottom seawater. Many of the major ions concentrations in spring fluids are indistinguishable from those of bottom seawater; however, concentrations of Rb, Mo, V, U, Mg, phosphate, Si and Li are different. Applying these observed differences to calculated global CHS fluxes results in chemical fluxes for these ions that are ≥15% of riverine fluxes. Fluxes of K and B also may be significant, but better analytical resolution is required to confirm this result. Spring fluids also have ~50% less dissolved oxygen (DO) than bottom seawater. Calculations of an analytical model suggest that the loss of DO occurs primarily (>80%) within the upper basaltic crust by biotic and/or abiotic consumption. This calculation demonstrates that permeable pathways within the upper crust can support oxic water–rock interactions for millions of years.

1. Introduction

Observed differences between measured and predicted lithospheric heat flux values from the deep seafloor are attributed to advective cooling of the crust by hydrothermal fluids (e.g., Lister, 1972). This process extracts ~10 TW (25%) of the Earth's lithospheric heat (Sclater et al., 1980; Stein and Stein, 1994; Mottl, 2003). Although high-temperature hydrothermal systems have been discovered and sampled at many seafloor spreading centers, where fluid flow at high temperatures (~250–400 °C) is driven by crustal cracking and the intrusion of magma (e.g., Corliss et al., 1979), such systems account for at most 20% of the global advective heat loss with the remainder occurring on ridge flanks at much lower temperatures (Mottl, 2003). In contrast, ridge flank hydrothermal systems are driven by conductive heat loss from the lithosphere. Sites of discharge and recharge in ridge flank systems are determined by (a) the permeability structure of the upper basaltic crust, (b) topographic relief, and (c) the distribution and properties of sediment above the crustal aquifer (e.g., Langseth et al., 1984; Davis et al., 1992; Fisher and Wheat, 2010). On ridge flanks, sediment acts as a low-permeability barrier that limits direct fluid exchange between the crustal aquifer and bottom seawater (Spinelli et al., 2004). In contrast, seamounts and other basaltic outcrops provide highly permeable channels for efficient fluid exchange between volcanic crustal rocks and the overlying ocean (e.g., Davis et al., 1992; Hutnak et al., 2008). Because the magnitude of ridge flank discharge is equal to the discharge of Earth's rivers to the ocean (Wheat et al., 2003), even a small change in the chemical composition of circulating fluids within the basaltic crust could impact global geochemical budgets (e.g., Elderfield and Schultz, 1996; Wheat and Mottl, 2004), yet no pristine samples of CHS fluids from ridge flanks have been collected.

* Corresponding author.
E-mail addresses: wheat@mbari.org (C.G. Wheat), afisher@ucsc.edu (A.T. Fisher), jmcmanus@bigelow.org (J. McManus), samiam0101@gmail.com (S.M. Hulme), borcutt@bigelow.org (B.N. Orcutt).

http://dx.doi.org/10.1016/j.epsl.2017.07.049

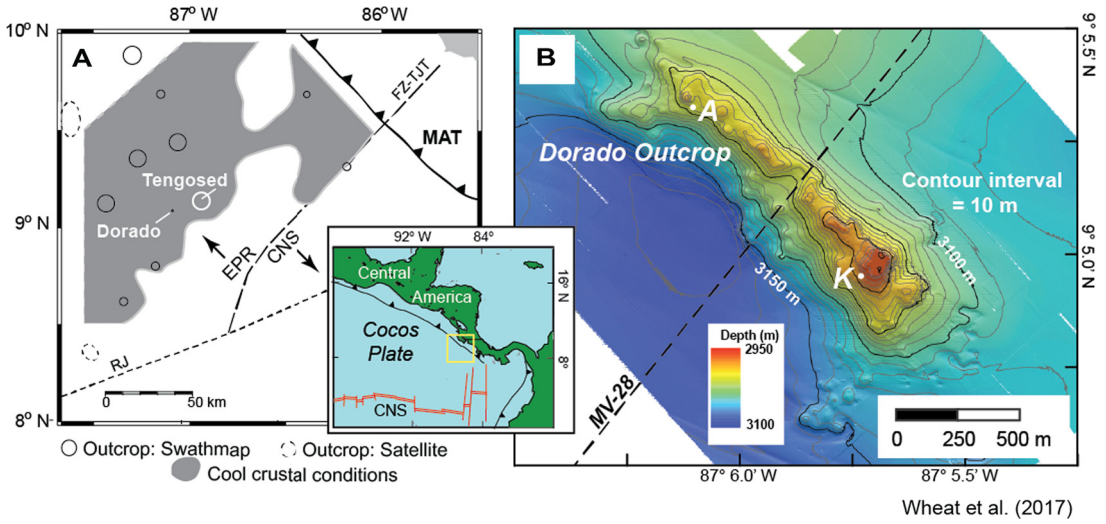

Fig. 1. A. Dorado outcrop is located on 23 M.y. old seafloor west of Costa Rica, on the Cocos Plate, in a region (gray area) where the heat flow is 10–40% of lithospheric predicted values, consistent with rapid hydrothermal circulation and advective heat loss (Fisher et al. 2003; Hutnak et al., 2008). Circles represent locations of know basaltic exposures, potential sites of fluid recharge and discharge. EPR – Lithosphere generated on the East Pacific Rise; CNS – Lithosphere generated on the Cocos-Nazca Spreading Center; RJ – Ridge Jump; MAT – Mid-America Trench; FZ-TJT – Fracture Zone-Triple Junction Trace. B. Bathymetric map of Dorado Outcrop from multibeam sonar data collected by the AUV *Sentry*. Contours are 10 m. The outcrop rises about 150 m above a sediment sequence that ranges from 200 to 400 m thick. "A" and "K" mark locations where long-term and numerous discrete fluid samples were collected. The dashed line shows the location of a seismic reflection profile (Fig. 2).

Much of the global ridge flank fluid flow occurs through young crust within cool (<20 °C) hydrothermal systems (CHS), where the difference between measured seafloor and lithospheric heat flux is greatest (Stein and Stein, 1994). In these regions, the lack of a continuous sediment cover allows many pathways for seawater to flow into and out of the volcanic oceanic crust. The ubiquity of basaltic exposure on many young ridge flanks (e.g., abyssal hills, fracture zones, seamounts and other outcrops; Macdonald et al., 1996) and the low temperature of discharge from CHS make it difficult to locate and sample fluids that are characteristic of these systems. Hydrothermal circulation on ridge flanks also occurs where thicker and more continuous sediment cover limits areas of basaltic exposure, resulting in slower fluid flow through the crust, longer residence times, and higher reaction temperatures (e.g., Mottl et al., 1998; Elderfield et al., 1999). However, the same processes and conditions that raise reaction temperatures during circulation result in a distinctive hydrothermal fluid composition that make these systems easier to locate and sample, but they are not globally representative, thus their global impact is limited (Mottl, 2003). Despite decades of searching, CHS on ridge-flanks have not been sampled, making it difficult to quantify the influence of ridge flank hydrothermal systems on crustal alteration and global geochemical fluxes.

On the eastern flank of the East Pacific Rise, on 18–23 M.y. old seafloor of the Cocos Plate (Fig. 1), the regional seafloor heat flux within a 14,500 km^2 area is 60–90% lower than lithospheric predictions (Fisher et al., 2003; Hutnak et al., 2007, 2008). Low values of conductive heat flux in this area are attributed to advective cooling as a result of vigorous hydrothermal circulation. Bathymetric mapping, seismic reflection, heat flux, and sediment pore water data were combined to identify areas of CHS recharge and discharge through basaltic edifices that penetrate up to 450 m of sediment in this area (Fisher et al., 2003; Spinelli and Underwood, 2004; Hutnak et al., 2007, 2008; Wheat and Fisher, 2008). Eleven basement highs were mapped in this region of low seafloor heat flux; one of the smallest basement edifices, Dorado Outcrop, was hypothesized to be a site of CHS discharge on the basis of heat flux measurements and the pore fluid geochemistry of sediments immediately adjacent to the outcrop (Hutnak et al., 2007; Wheat and Fisher, 2008). However, these surveys with conventional oceanographic vessels could not identify sites of direct CHS discharge, and neither did they permit sampling of pristine CHS fluids.

Fluids that discharge from Dorado Outcrop are thought to have recharged through Tengosed Seamount, located ~20 km to the east, where there are anomalously low heat flux values adjacent to the edge of the seamount (Hutnak et al., 2007, 2008). Thermal and sediment pore water geochemical data from earlier surveys, and one-dimensional analytical models of coupled fluid-heat and fluid-solute transport, suggest that upper basement temperatures are ≤20 °C between Tengosed and Dorado, and that fluid flow is rapid, with a fluid residence time in the basaltic crust of 0.6 to 3 y (Wheat and Fisher, 2008; Hutnak et al., 2008). Laboratory studies of seawater–basalt interactions at low temperatures (25 °C) indicate slow reaction rates (Seyfried, 1977). Thus, the low upper-crustal temperatures and the short residence time of fluids discharging from Dorado Outcrop should result in a fluid composition that is only slightly modified from bottom seawater, but even small changes in fluid composition could result in globally significant geochemical fluxes because of the enormity of such discharge from the oceanic crust. Thus, given that the Dorado Outcrop is located in a ridge-flank setting where the basaltic crust is generally covered with thick sediments, much of the lithospheric heat is lost to advection in this region, and there are only a few sites of basaltic exposure where such hydrothermal exchange could occur with bottom seawater, the Dorado Outcrop was a promising target for locating and sampling fluids that discharge from CHS.

On this basis, we embarked on two expeditions to Dorado Outcrop to locate sites of CHS discharge and collect the first pristine samples of CHS fluids from a ridge flank. The first expedition (AT26-09) focused on the use of the autonomous underwater vehicle *Sentry* and the remotely operated vehicle *Jason II*, to map the outcrop, survey the area for springs, and sample spring sites. Long-term instruments were deployed to measure discharge temperatures and collect spring fluids. A second expedition (AT26-24), about one year later, recovered these instruments and collected additional samples at spring discharge sites with the submersible *ALVIN*.

2. Methods

2.1. Bathymetric data

Bathymetric data were collected by the AUV *Sentry* using a Reson Seabat 7125 400 kHz multibeam sonar at an elevation of ~50 m above the seafloor. Data were processed using MBSystem (Caress et al., 2008) in conjunction with a series of MATLAB programs (McCue and Yoerger, 2010). *Sentry* navigation data from the Doppler Velocity Log (DVL), inertial navigation system (INS), and Ultra-Short Base Line (USBL) were merged and combined with Reson s7k multibeam data files. The navigated multibeam data were filtered and visually inspected for anomalous pings prior to producing a preliminary bathymetry map. Due to the steep topography and irregularities with the USBL positioning, the navigation was subsequently manually corrected by selecting morphologic tie-points from overlapping swaths and applying a statistical fit to the AUV navigation using the program MBNavAdjust. Processed multibeam data were gridded at a resolution of 1 m using a near-neighbor algorithm. Data are archived on NCEI in accordance with standard practices including raw, processed, and gridded files (Hulme, 2015).

2.2. Discrete fluid samples and sensor collection

Discrete measurements of temperature were made with standard thermal couples mounted on *Jason II* and *ALVIN*. Discrete dissolved oxygen (DO) concentrations were measured with an Aanderra optode connected to electrical penetrators on the submersible *ALVIN*, providing a continuous readout within the submersible. When possible, an inverted polyvinyl chloride (PVC) funnel was positioned above a spring to focus fluid discharge before measurements were made. Only after confirming the warmest temperatures or low dissolved oxygen concentrations were discrete fluid samples collected.

Discrete fluid samples were collected using a novel sampler by placing a sampler inlet directly in shimmering spring discharge or within the opening of an inverted funnel, which was used to minimize seawater entrainment during sampling. Squeezing the actuator with the manipulator on the submersible triggered these samplers. The trigger released a spring attached to a piston in a ~200 ml syringe. The portion of the sampler that was in contact with the sample was made from polycarbonate and Pyrex glass. A one-way valve and 1/8-inch inner diameter (ID) tubing was attached to the intake of the syringe to minimize exchange with seawater during continued submersible operations and recovery. The tubing also served to slow the rate of sample uptake, minimizing dilution with bottom seawater during collection. The dead volume from the syringe plunger and intake tubing was 2 ml. Before each deployment, syringes were acid cleaned with 10% HCl, rinsed three times with 18 MΩ distilled water, and rinsed three times with filtered bottom seawater. Upon recovery, discrete samples were filtered using 0.45 µm-mesh and aliquoted into hot-acid-washed high-density polyethylene bottles, glass ampules, and glass vials.

2.3. Continuous fluid samplers and data collection

Continuous fluid samplers (OsmoSamplers, Jannasch et al., 2004) were deployed with *Jason II* for one year to sample spring fluids. These samplers were configured with a 12-membrane pump and a 300-m-long coil of Teflon tubing. The small-bore tubing (1.1 mm ID) was initially filled with 18 MΩ water to maintain a constant "pump" rate with time. OsmoSamplers were configured with a tee-handle that contained the end of the small-bore Teflon (sample) tubing within a protective polycarbonate tip that was further protected within a stainless steel wand attached to a tee-handle. This allows us to place intakes deep within cracks and gaps in the rock from which fluids discharge, where discrete samplers cannot reach. OsmoSamplers were recovered approximately one year after deployment and processed at sea (Wheat et al., 2011). Teflon coils were cut in 1.1 m lengths and 1.2 ml of fluid was expelled from each length of tubing into hot-acid-cleaned plastic microcentrifuge tubes. A portion of these aliquots were acidified with subboiled HCl to a pH of ~1.8.

Continuous temperature records were collected using autonomous temperature sensor/loggers with a range of −40 to 125 °C and 12-bit resolution (Onset U12-015, titanium), equivalent to a precision of ±0.02 °C at typical temperatures measured in this study. Dissolved oxygen concentrations were measured with a prototype of the *soloDO* logger (RBR Ltd., Canada), comprising an Aanderra optode and an integrated temperature sensor.

2.4. Chemical measurements

Alkalinity was determined potentiometrically at sea via titration with 0.1N hydrochloric acid; a pH measurement was conducted as part of this procedure. Inductively coupled plasma optical emission spectrometry (ICPOES) was used on shore to measure Na, Mg, Ca, K, Sr, Li, and S with a 1:200 dilution and Sr, Li, Fe, Mn, and B with a 1:25 dilution in 1% nitric acid. Inductively coupled plasma mass spectrometry (ICPMS) was used to analyze Rb, Cs, Ba, Mo, V and U with a 1:75 dilution in 3% nitric acid. Nutrients (silicate, phosphate, nitrate, and nitrite) were measured on shore and nitrate was measured at sea using standard colorimetric, automated, flow injection analysis procedures (Armstrong et al., 1967; Atlas et al., 1971; Bernhardt and Wilhelms, 1967; Gordon et al., 1994; Patton, 1983).

Chlorinity and Ca were determined potentiometrically via titration with silver nitrate and EGTA, respectively. Mg was measured using a standard colorimetric titration method using EDTA. Ca and Mg titrations were conducted only on discrete samples. Sediment pore water DO was measured at sea with a needle-type oxygen optode inserted radially into sediment gravity cores and push cores collected by *ALVIN* (e.g., Orcutt et al., 2013).

All chemical and thermal data are provided in the Supplemental Material. Also included in these tables is a measure of the composition of bottom seawater that is based on the average value of six to twenty-four measurements of bottom seawater collected from Niskin samples on three dives. The uncertainties associated with these average bottom seawater values indicate the potential errors associated with sample handling, processing, and instrument precision (Table 1).

3. Results and discussion

3.1. Dorado Outcrop geology and fluid temperatures

A high-resolution bathymetric map of Dorado Outcrop and the surrounding area was compiled from data collected with *Sentry* (Fig. 1). Dorado Outcrop rises 100–150 m above the surrounding sediment plain, and is exposed as an elongated edifice trending southeast-northwest that is 0.5 km wide and 2 km long. The outcrop is composed primarily of basaltic pillows and sheet flows and is bounded on the southeast side by a near-vertical 80–100 m-high scarp. There is a topographic saddle near the middle of the outcrop that separates two bathymetric highs and appears to have been formed by the partial collapse of the western side of the edifice, with transport of rubble to the southwest. The seafloor surrounding Dorado Outcrop is generally flat, but there is a depression ~20–30 m deeper than the surrounding seafloor, ~400 to 500 m

Table 1
Concentrations of bottom seawater and spring fluids and calculated fluxes.[a]

	Bottom SW Ave ± stdev	Spring fluid Ave ± stdev	% of river flux
Temperature °C	1.85 ± 0.004	12.3 ± 0.01	–
Dissolved O_2 µM	108 ± 0.1	54.5 ± 0.1	–
pH	7.76 ± 0.03	7.80[b]	–
Alkalinity mmol/kg	2.42 ± 0.01	2.47[b]	−1
Mo nmol/kg	115 ± 2	126 ± 2	−26
V nmol/kg	37.3 ± 0.5	76 ± 1	−30
Rb nmol/kg	1250 ± 6	1310 ± 20	−80
U nmol/kg	13.1 ± 0.3	11.7 ± 0.2	+18
Li µmol/kg	26.2 ± 0.3	25.1 ± 0.1	+36
Ba nmol/kg	150 ± 1	146 ± 2	+0.2
PO_4 µM	2.69 ± 0.07	1.99[b]	+15
Silicate µM	156 ± 5	198 ± 4	−3
Mg mmol/kg	52.9 ± 0.2	52.2[b]	+61
Ca mmol/kg	10.27 ± 0.04	10.18[b]	+3
B µmol/kg	400 ± 4	404[b]	
K mmol/kg	10.1 ± 0.1	10.12 ± 0.02	
Na mmol/kg	466 ± 5	465 ± 2	
S mmol/kg	27.9 ± 0.3	27.8 ± 0.1	
Chlorinity mmol/kg	540.9 ± 0.5	542 ± 3	
NO_2 µM	0.08 ± 0.01	0.02[b]	
$NO_3 + NO_2$ µM	38 ± 1	38[b]	
Cs nmol/kg	2.19 ± 0.04	2.24 ± 0.5	
Mn µmol/kg	<0.1 ± 0.03	<0.1	
Fe µmol/kg	<0.2 ± 0.16	<0.2	

[a] The calculated percent of the river flux is based on a global heat loss of 8.1 TW, a thermal anomaly of 13.2 °C above ambient, and riverine fluxes (Elderfield and Schultz, 1996). Positive fluxes are into the oceanic crust.
[b] Results are based on discrete sample data.

across, on the western side of the outcrop, presumably generated from sediment scouring by bottom currents.

Exploration for hydrothermal springs on Dorado Outcrop focused initially near the top of the edifice where linear cracks were discovered in the basaltic crust. Some of these cracks are tens to hundreds of meters long and, in general, follow the trend of the outcrop. However, we found little evidence for fluid discharge associated with such features. Three sites of fluid discharge were subsequently discovered where "shimmering" water emerged from smaller cracks and the margins between pillow flows. Two of the high discharge areas are indicated by Markers K and A. The third site is located along the southeastern margin of the outcrop, just above the sedimented seafloor, but discharge was less vigorous in 2014 and no fluid samples were collected from this site in 2014. CHS discharge at these sites was associated with observations of octopuses, shrimp, fish, crabs, and small worms.

Temperature measurements were made using a manipulator-mounted probe in and around shimmering water that discharged from the outcrop (Table 1, Supplemental Material). The most vigorous fluid discharge occurred at Marker K (Fig. 1) where shimmering water exits ubiquitously from cracks and gaps between pillows that covered an area of several hundred square meters. The maximum temperature measured with discrete and continuous sensors was 12.3 °C, well above the bottom seawater temperature of 1.85 °C. Yet significant variations were observed in measured temperatures and visual estimates of the rate of fluid discharge during multiple visits to individual spring sites. For example, the spring sampled at Marker A (Fig. 1) was discharging 11.6 °C fluid in December 2013, but there was no discharge apparent upon the initial return in December 2014. However, six days later, 7.6 °C fluids discharged from Marker A. This suggests that basement permeability is relatively high, being modulated by variations in tidal pressure, consistent with inferences drawn from the very low heat flux around Dorado Outcrop and on other parts of the EPR-generated Cocos Plate in this region (Fisher et al., 2003; Hutnak et al., 2007, 2008).

Estimates for the temperature at the sediment–basement interface around Dorado Outcrop, and, by supposition, the temperature of hydrothermal fluids in the upper basaltic crust (formation fluid), were made using seismic reflection and seafloor heat flux data collected during earlier surveys with surface ships (Hutnak et al., 2007; Fisher and Harris, 2010), using the method of Davis et al. (1999) (Fig. 2). Seismic data were used to calculate the sediment thickness and thermal resistance of the sediment column, using physical properties from nearby drilling sites, and co-located heat flux measurements were extrapolated downward to the sediment–basement interface by one-dimensional boot-strapping (Hutnak et al., 2007). This approach results in calculated temperatures at the sediment–basement interface in the region around Dorado Outcrop of 15–20 °C, with a value west of Dorado Outcrop of ~15 °C (Fig. 2). This temperature is several degrees warmer than the highest temperature measured in discharging fluids from springs on Dorado Outcrop, suggesting that hydrothermal fluids cool conductively during ascent from depths of the upper permeable basaltic crust, which is generally buried by 200–400 m of sediment in this region (Spinelli and Underwood, 2004; Hutnak et al., 2007). Conductive heat loss during fluid ascent was also observed at Baby Bare outcrop, the host of a ridge flank hydrothermal system on the eastern flank of the Juan de Fuca Ridge (Wheat et al., 2004). Such conductive heat loss during fluid ascent within the crust is commonplace at hydrothermal discharge sites more generally (e.g., Corliss et al., 1979).

3.2. *Composition of the formation (spring) fluid within the basaltic aquifer*

Defining the composition of fluid discharging from Dorado Outcrop proved to be challenging because compositional differences between these fluids and bottom seawater are small, and bottom seawater was often entrained during sampling. The latter complication is typically addressed in studies of higher-temperature, seafloor hydrothermal systems by cross-plotting ions and applying a conservative mixing model defined by two end-members: crustal formation fluids and bottom seawater. Concentrations of Mg are typically used with this method because Mg tends to be almost completely depleted in hydrothermal fluids that react with basalt at elevated (>60 °C) temperatures (Fisher and Wheat, 2010). However, in low temperature hydrothermal fluids, such as those that discharge from Dorado Outcrop, concentrations of Mg are typically less than the bottom seawater value but are minimally altered relative to bottom seawater. Thus, the concentration of the discharging fluid cannot be determined using this common approach.

Another approach for determining the composition of spring fluids in high-temperature systems is to plot ion concentrations versus fluid temperature, again based on the assumption that pristine hydrothermal fluids tend to mix conservatively with entrained bottom water, then extrapolate to the inferred *in situ* temperature in the volcanic crust. This method fails for fluids sampled from Dorado Outcrop because we cannot assume an adiabatic rise from depth – heat is not conserved and lost to the surrounding crust by conduction. Additional evidence for conductive cooling during the ascent of formation fluid from Dorado Outcrop is apparent in the continuous temperature records with corresponding chemical records at Marker K (Fig. 3). Year-long records of chemical data from OsmoSamplers, which integrate fluid collected during intervals of ~1.5 day, and the multi-day, 5-min resolution DO data display minimal variations in concentration with time, yet spring temperatures vary significantly on diel and longer time scales, consistent with tidal modulation of discharge rate. Because ionic diffusion is orders of magnitude slower than thermal conduction (diffusion) time-varying discharge can result in large differences in the temperature of ascending fluid, whereas the geochemical com-

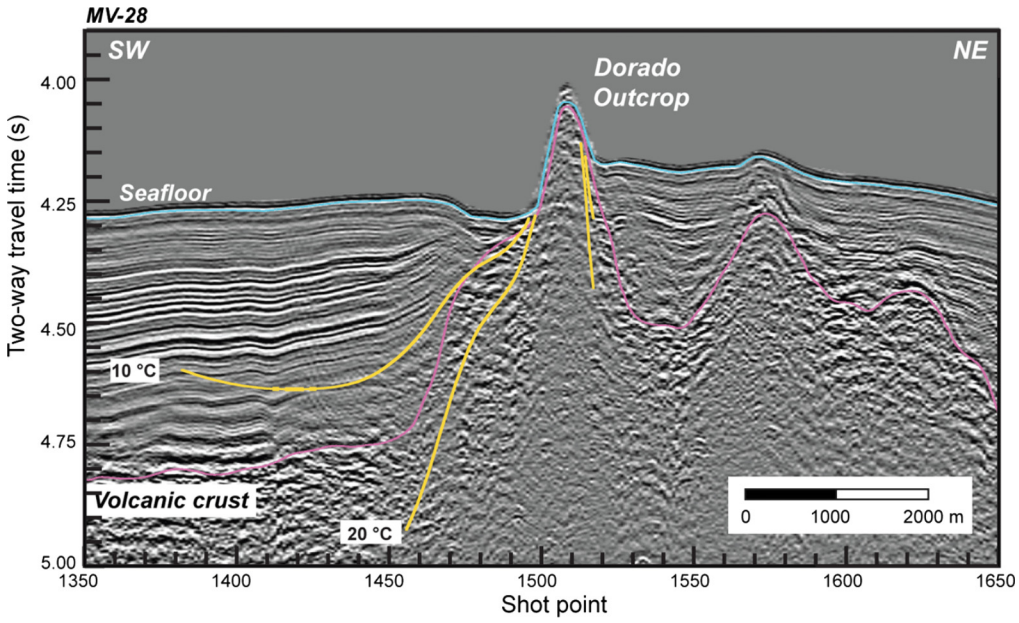

Fig. 2. Map of isotherms within the oceanic crust near Dorado outcrop based on single channel seismic and co-located heat flux data. The blue line delineates the seafloor, the pink line delineates the sediment–basement interface and the yellow lines are isotherms that are based on projecting the seafloor heat flux measurements to depth within the crust. The outcrop is about 150 m high with scouring of the sediment to the west. Sediment thickness to the west of the outcrop is about 400 m thick.

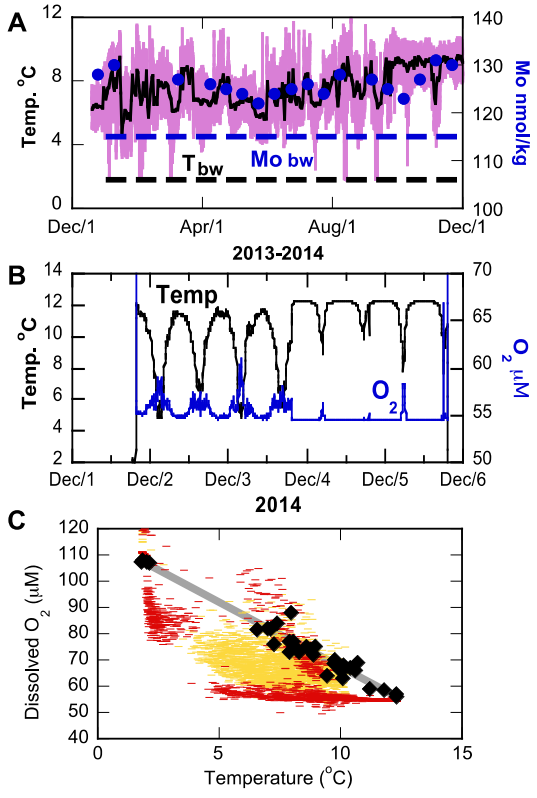

Fig. 3. Temporal variability in the thermal and chemical composition of spring fluids at Dorado Outcrop. A. Year-long record of temperature (purple), daily running average temperature (black), and Mo concentrations from spring fluids (blue circles) and bottom seawater values (dashed horizontal lines) illustrate long-term fluctuations in spring fluid composition at Marker K. B. Temperature and dissolved oxygen (DO) record from a four-day period at Marker K, highlighting daily changes in response to variations in discharge rate and mixing with bottom seawater. C. Discrete and sensor spring DO concentrations from Dorado Outcrop plotted as a function of temperature. The gray line is the best-fit linear regression to the discrete measurements, which were collected from spring sites on the outcrop (black diamonds). Data from *in situ* sensors (red and yellow bars from two different orifices in the Marker K area) highlight the effects of varying flow and entrainment rates during four deployments (two at each site), each lasting 3 to 4 days.

position of the same fluid changes little with time. DO-temperature trends from the continuous data set (Fig. 3C), which are influenced by changes in flow rate and variable mixing with bottom seawater, are distinct from discrete measurements that were collected by pushing sampler inlets into the most vigorous flow to get the most pristine samples. Similar variations in temperature relative to fluid composition were observed in warm springs that discharge from Baby Bare outcrop (Wheat et al., 2004).

We define the chemical composition of the formation fluid that discharges from Dorado Outcrop using three approaches that depend on the type and quantity of sample and data collected and the difference in concentration relative to bottom seawater. First, the concentration of DO in formation fluids was defined by *in situ* sensor measurements, which are contemporaneous with thermal measurements, and discrete measurements that were followed or preceded by discreet thermal measurements (Fig. 3). Time-series DO concentrations during warm conditions were 54.5 ± 0.1 μM (±1 standard deviation of the time-series data), when measured temperatures were ≥11 °C (Table 1). This corresponds to the lowest DO concentration measured with the discrete sensor, and the highest measured temperatures (Fig. 3). We interpret these combined datasets to indicate that the highest fluid temperatures are the most representative of crustal DO concentrations within and below Dorado Outcrop. These data indicate that the formation fluid must be oxic, because extrapolating the mixing trend for DO and temperature (Fig. 3C) to 0 μM DO would indicate a formation temperature of ~23 °C, higher than indicated by downward continuation of seafloor heat flux data (~15 °C, Fig. 2).

A second means to define the composition of the formation fluid is through the analysis of small fluid samples (~1.2 mL) collected with OsmoSamplers. We report the average value and standard deviation for samples collected with the OsmoSampler that was deployed at Marker K (Fig. 3, Table 1, Green OsmoSampler Supplementary materials). A temperature recorder that was deployed with this OsmoSampler showed consistently elevated temperatures throughout the year-long deployment (average ~8 °C with sustained periods at ~12 °C; Fig. 3). Chemical data from this OsmoSampler show consistently uniform concentrations for several elements that are distinct from bottom seawater (e.g., Mo values shown in Fig. 3A). However, because hydrothermal discharge rates

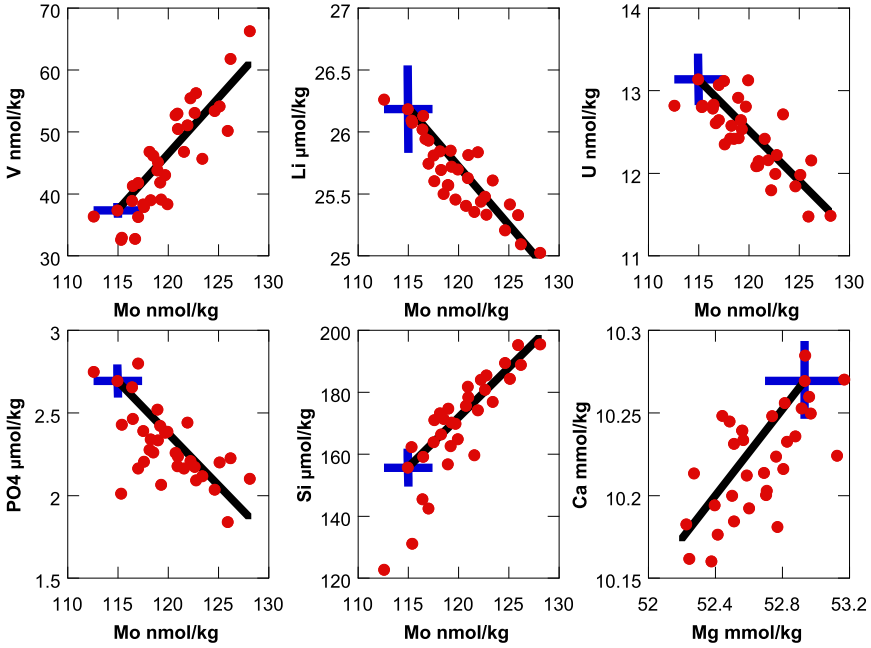

Fig. 4. Representative data from discrete samples (Data are listed in the Supplemental Material). Discrete data highlight geochemical differences between bottom seawater (blue cross is ±1□ about the average) and spring fluid (red circles). The best-fit line (black line) is a linear regression that is forced through bottom seawater.

varied with time, and there could be some entrainment of bottom seawater with these samples, we consider differences between these samples (OsmoSamplers) and bottom seawater to represent minimum deviations in the composition of the formation fluid relative to bottom seawater. In the case of Mo, the apparent concentration in discharging fluids is 126 ± 2 nmol kg^{-1}, whereas the Mo concentration in bottom seawater is 115 ± 2 nmol kg^{-1} (Fig. 3a, Table 1).

The third method for calculating the composition of the formation fluid uses data from the discrete samplers, particularly samples that were collected using an inverted funnel placed over discharging springs. The concentration for the formation fluid based on these discrete samples was calculated by linear extrapolation with Mo through the seawater value (Fig. 4) and calculated for 126 nmol Mo/kg formation fluid concentration, which is the average concentration of the year-long record from the OsmoSampler (Fig. 3). Mo was used as a reference for empirical reasons; its concentration is significantly altered relative to bottom seawater, and the average Mo concentration from the OsmoSampler was matched by the most altered (pristine) samples collected with discrete samplers.

We had to apply these combined methods to determine the spring fluid composition because differences in the spring and bottom seawater concentrations are on the order of the analytical precision. For example, concentrations of Mg and Ca are within $\pm 1\sigma$ of the bottom seawater value in the year-long (OsmoSampler) record, as determined by ICPOES techniques (Supplemental materials). However, both elements may be slightly depleted relative to seawater, based on the discrete samples that were analyzed using the more precise analytical method of titration (Fig. 4). While concentrations for most of the major ions in spring fluids from Dorado Outcrop are virtually indistinguishable from those of bottom seawater, some solutes are distinctly different, including Rb, Mo, V, U, Mg, phosphate, Si and Li (Table 1). Notably, the effort required to define a crustal hydrothermal end-member fluid based on application of multiple sampling and measurement techniques, including the use of Mo as a geochemical reference, highlights the challenges inherent in the collection and analysis of fluids from a CHS.

3.3. Removal of dissolved oxygen (DO) in the basaltic aquifer

The concentration of DO in spring fluids is ~50% the value of bottom seawater in this area (Table 1, Fig. 3). The loss of DO must occur between the time that bottom seawater recharges at Tengosed Seamount (or another, more distant site) and travels laterally through the volcanic crustal aquifer to discharge at Dorado Outcrop. Inflow of bottom seawater is thought to occur mainly around Tengosed seamount, the nearest known site of seawater recharge, as indicated by localized suppression of seafloor heat flux (Hutnak et al., 2007, 2008). More specifically, recharge is thought to occur around the base of Tengosed Seamount where the integrated density of the water column, which drives the hydrothermal siphon, is greatest, consistent with seafloor heat flux measurements (Hutnak et al., 2007) and radial and three-dimensional simulations of flow through large seamounts (Winslow and Fisher, 2015; Winslow et al., 2016). Processes contributing to the loss of DO in advecting formation fluids include: diffusive exchange with overlying sediment pore fluids, abiotic water–rock reactions, and microbial metabolic activity. The relative contribution of these three processes to DO loss from basement fluids are considered in this section.

There should be some loss of DO from the basaltic aquifer to the overlying sediment pore waters by diffusion because microbial respiration consumes oxygen in the sediment (Fig. 5B). Because there is no source of DO in the sediment and the underlying formation fluids have DO in the range of 108 µM (bottom seawater) to 54.5 µM (spring fluids) (Table 1), there must be some diffusive loss of DO from circulation fluids in the basaltic aquifer to the overlying sediment pore waters. However, the relative magnitude of this diffusive loss may be small or not measurable if the DO flux associated with the rapid advective lateral fluid flow through the basaltic aquifer is significantly greater than the diffusive flux.

To assess the magnitude of these two transport terms, we apply a one-dimensional model of simultaneous diffusion and advection (Fig. 5A), as used previously to assess fluid flow in basement rocks based on pore fluid profiles within overlying sediment (Wheat and Fisher, 2007, 2008; Orcutt et al., 2013). Parameters for these calculations included bottom seawater and spring fluid DO concentrations (Table 1), an estimate for the diffusive flux at the

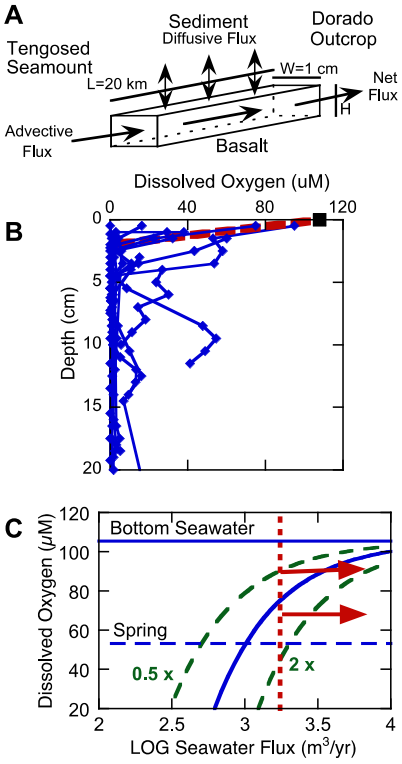

Fig. 5. Model simulations for dissolved oxygen (DO) data from Dorado Outcrop. A. A transport-reaction model was used to calculate the DO concentration of the spring fluid, given a volumetric flux per centimeter width perpendicular to flow, bottom seawater concentration (solid blue horizontal line in C), distance traveled, and a diffusive flux across the sediment–basement interface (modified from Wheat and Fisher, 2007). B. Sediment pore water DO data. The gradient at the sediment-water interface (red dashed line) was used to define the diffusive flux based on pore water data (blue symbols and lines) and the concentration in bottom seawater (black square). C. Model calculations based on the DO gradient shown in B (solid blue curve) and values that are calculated using one-half and twice this DO gradient (dashed green curves). The vertical red dashed line is the minimum volumetric flux based on constraints dictated by the nitrate data, consistent with earlier results (Wheat and Fisher, 2008). Arrows point towards flow conditions that are more likely for this area. Given that the DO gradient is likely to be less at the sediment basement interface than at the seafloor (Orcutt et al., 2013), most (>80%) of the DO loss is accounted for by reaction within the upper basaltic crust, not diffusion to the overlying pore waters. This consumption is by biotic or abiotic reactions or both.

sediment-basalt interface based on sediment pore water DO profiles (Fig. 5B), the lateral distance across which flow occurs, and the volumetric fluid flux perpendicular to flow in basaltic crust. We estimate the maximum upward diffusive flux of DO across the sediment–basement interface based on pore water DO concentrations in gravity and push cores collected on and near Dorado Outcrop. These pore waters are typically depleted in DO at a depth of ~2 cm, but several cores indicate a decrease in DO followed by an increase in DO with depth (Fig. 5B). Such profiles are consistent with a diffusive flux of DO from the crustal aquifer (Ziebis et al., 2012; Orcutt et al., 2013). On the basis of the near surface DO profiles, we estimate a diffusive gradient at the seafloor of 54 μM DO cm^{-1} (Fig. 5B). This gradient is an upper limit, because the DO gradient near the sediment–water interface is 2 to 6 times greater than the gradient at the sediment–basement interface in a similar hydrologic and sedimentary organic matter setting, the cool ridge flank hydrothermal system at North Pond on the western flank of the Mid-Atlantic Ridge (Orcutt et al., 2013).

Given these gradients, model calculations show how the diffusive loss of DO in basement fluids depends on the lateral fluid flow rate between Tengosed Seamount and Dorado Outcrop (Fig. 5C). For diffusion alone to explain a loss of ~50% of the DO in formation fluids, the flow rate must be ~1000 $m^3\,y^{-1}\,cm^{-1}$ perpendicular to flow. However, prior calculations for this area based on sediment pore water nitrate data suggested a minimum flow rate on the order of 1800 $m^3\,y^{-1}\,cm^{-1}$, consistent with the formation fluid having the same nitrate concentration as bottom seawater (Wheat and Fisher, 2008) (Table 1). Using the minimum fluid flux calculated from the nitrate data, the DO concentration from bottom seawater at the presumed point of entry at the nearest recharge site, Tengosed Seamount, and the diffusive DO gradient to the overlying sediment pore waters, the calculated spring water DO concentration is 75 μM, about 20 μM higher than measured. This calculation suggests that ~60% of the DO loss from the formation fluid could be explained by upward diffusion into the overlying sediments (Fig. 5C). The remainder must be consumed by reactions within the basaltic aquifer, by biotic and/or abiotic processes.

In practice, these calculations are likely to over-estimate the diffusive loss of DO from crustal formation fluids to overlying sediment. If the DO gradient at the sediment–basement interface were only half of the gradient at the seafloor, which would be more consistent with the difference in measured gradients from North Pond (Orcutt et al., 2013), then only 30% of the DO loss could result from diffusive exchange with the overlying sediment pore waters. Given that the volumetric flux based on the nitrate data is a minimum value, and given that oxygen consumption at the sediment basement interface is likely to be much less than that at the seafloor, it seems likely that most of the DO removal in formation fluids occurs as a result of processes other than diffusion into the overlying sediment. We cannot empirically differentiate between abiotic oxidation of mineral surfaces and microbially driven oxidation within basement rocks, but considering the low temperature of the upper basaltic crust in this area, sluggish abiotic reactions at these temperatures (Seyfried, 1977), and a nominal travel time from Tengosed to Dorado Outcrop of 0.6 to 3 y (Wheat and Fisher, 2008), much of this DO consumption is likely to be mediated microbially.

3.4. Chemical fluxes to the ocean and crust at cool hydrothermal springs CHS)

The CHS fluids sampled at Dorado Outcrop clearly differ from bottom seawater in temperature, dissolved oxygen (DO), Li, phosphate, Rb, Mo, V, U, Mg, and silicon and may differ in pH, alkalinity, Ba, and Ca (Table 1). We use these differences in fluid composition to calculate fluxes of these ions to or from the crust as the global component from ridge-flank CHS. These calculations are based on the assumption that fluids collected at Dorado Outcrop are characteristic of CHS systems in general. The global fluid flux is heavily weighted to low temperature environments (Wheat et al., 2003), and that low temperature fluids likely have a short residence time within the crust (Johnson and Pruis, 2003). Although the geological setting at Dorado Outcrop may be somewhat atypical of young-cool, ridge-flank hydrothermal sites (i.e., isolated basement outcrops on 23 M.y. old seafloor extending through regionally thick and continuous sediments, as opposed to mostly unsedimented ridge flank), the key parameters that control the extent of reaction within the basaltic crust are the temperature of reaction and the residence time of the fluid in the volcanic crust. Both of these values are low for CHS sampled at Dorado Outcrop, as they should be globally. Given the difficultly in locating discharge in young lightly sediment crust, data from Dorado Outcrop provide a reasonable means to assess the magnitude of CHS chemical fluxes to and from the crust.

Given the measured chemical anomalies in discharging fluids from Dorado Outcrop, a global heat loss of 8.1 TW (Mottl, 2003), and a thermal heating of ~13.2 °C (formation temperature minus bottom water temperature), calculated fluxes are >15%

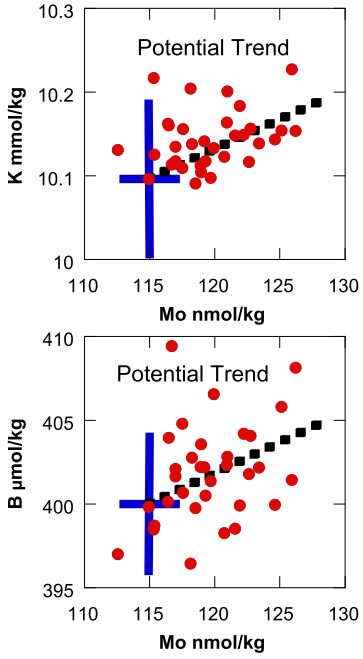

Fig. 6. Discrete data highlight geochemical differences between bottom seawater (blue cross is ±1□ [standard deviation] about the average) and spring fluid (red circles). The best-fit linear regression (black dash) is forced through bottom seawater with an r value that is statistically different from 0 (no correlation). The means and standard deviations of the seven samples with the highest Mo concentrations, representing samples of hydrothermal fluids with the least amount of mixing with bottom seawater during and prior to sample collection, are statistically different from bottom seawater ($\alpha = 0.05$ from a t-test utilizing means and standard deviations of bottom seawater and the seven samples). Thus, statically the concentrations of K and B are greater than the values in bottom seawater. These data indicate potential trends that would be significant to global fluxes and highlight the need for high quality samples and more precise analytical methods to better quantify such fluxes for these elements.

of the riverine fluxes for Mo, V, U, Li, Rb, phosphate, and Mg (Table 1). These results are similar to and consistent with previous estimates based on pore water data (Wheat and Fisher, 2008); however, estimates based on measurements of spring fluid samples are more reliable because these samples are less susceptible to sampling artifacts compared to pore water collection (e.g., K; De Lange et al., 1992), and pore waters are exposed to environment factors such as possible abiotic and biotic reactions that can alter the fluid composition as pore fluids ascend the sediment column. The biggest uncertainties in these calculations are associated with the chemical compositions of sampled fluids, as discussed below. The temperature of reaction could be greater if flow were deeper into the crust and poorly mixed (e.g., Anderson et al., 2013), but then we would expect to collect more reacted fluid than observed at Dorado Outcrop, and seafloor heat flux suppression would also be commensurately lower.

Some of differences in composition between discharging spring fluids from Dorado Outcrop and bottom water are indeed quite small, yet they can have a significant impact on oceanic budgets because the global discharge of CHS fluid is so large. Based on fluids from Dorado Outcrop that were collected with OsmoSamplers, concentrations of K, B, Ca, and Mg are statistically indistinguishable from bottom seawater. However, the discrete samples that are the most different from bottom seawater have concentrations of K and B that are distinctively different (Fig. 6). There may also be weak trends in cross-plots of K and B versus Mo, indicating the extent of mixing between CHS fluids and bottom water. If chemical anomalies for these two ions were just 1% different from seawater (well within sampling and measurement uncertainties) then global CHS fluids could contribute to K and B fluxes that are >25% of riverine fluxes. Likewise, there is a small difference (1.3%) between Mg concentrations in Dorado Outcrop spring fluid and bottom seawater, based on the titration method. This difference results in a calculated Mg flux for CHS fluids that is ~61% of the riverine flux. These calculations highlight the potential significance of ridge-flank processes for these elements and the need for high quality samples and accurate analytical techniques to resolve the nature and magnitude of chemical fluxes from CHSs in general.

Comparison of these estimated global fluxes with independent observations from the rock record increase our understanding of crustal processes. For example, iron oxidation within the oceanic crust, based on analysis of basaltic samples recovered from scientific ocean drilling, consumes $1.7 \pm 1.2 \times 10^{12}$ mol O_2 y^{-1}, and S oxidation consumes $1.1 \pm 0.7 \times 10^{11}$ mol O_2 y^{-1} (Bach and Edwards, 2003). These calculations included the reduction of nitrate, yet nitrate consumption is not apparent in CHS fluids recovered from Dorado Outcrop. Based on the DO data from Dorado Outcrop and the calculated global fluid flux from CHS, the calculated global oxygen consumption rate is 2.5×10^{11} mol O_2 y^{-1}, accounting for ~10% of that observed in the rock record. Thus, to match the rock record, the average global CHS must be cooler than 15 °C, because this would require an even larger fluid flux to remove the 8.1 TW of heat (Mottl, 2003), and/or younger crust (<10 M.y.) must be more reactive than the ~23 M.y. old crust around Dorado Outcrop (e.g., Staudigel et al., 1981). Some studies have suggested that reactions within the basaltic crust largely cease at 10 to 20 M.y. (e.g., Staudigel et al., 1981; Bach and Edwards, 2003; Coogan et al., 2016), based on material recovered through deep-sea scientific drilling. However, recovery in the upper volcanic crust is typically only 10–30%, and is heavily biased towards more massive and well-cemented units, which will tend to under-sample the portion of the upper crust through which the most rapid, low-temperature fluid flow is likely to occur. Results from this study show that reaction within the upper basaltic crust can occur in crust older than 20 M.y. Although the significance of such reactions on a global scale is not well constrained from this singular dataset, results from Dorado Outcrop illustrate the importance of direct sampling of low-temperature hydrothermal fluids in other yet to be discovered ridge flank settings to resolve the scale of their impact.

Changes in crustal fluid composition during CHS transport around Dorado Outcrop result from either water–basalt reaction, microbial activity within basaltic crust, and/or diffusive exchange with overlying sediment pore waters. For each of the ions listed above, measured chemical anomalies are consistent with reactions within the basaltic aquifer dominating the extent of the anomaly, because diffusive gradients of these ions in pore fluids are much less than the gradient defined by the DO data. Thus model calculations are consistent with minimal diffusive loss to the overlying pore fluids during rapid lateral fluid flow within the basaltic aquifer. Examples of potential reactions within the basaltic crust include secondary mineral (clay) formation that removes alkali metals (Li, K, Rb, and Cs) from circulating fluids (e.g., Staudigel et al., 1981; Hart and Staudigel, 1982). Li is clearly depleted in spring fluids (Table 1); however, Rb is enriched, K may be enriched (Fig. 6), and Cs is within the uncertainty of the analyses. Likewise, the increases in silicon likely result from release during clay formation and/or during the oxidation of ferrous iron-bearing silicate minerals and mesostasis to iron oxyhydroxides. Iron oxides have an affinity for removing the oxyanions P and U from seawater, consistent with spring data (Feely et al., 1998; Wheat et al., 2003). The alkalinity increase is consistent with clay formation, and the lower Ca values would indicate carbonate formation, which was observed in basalt samples that were recovered from areas bathed in fluids that discharge from Dorado Outcrop.

4. Conclusions and significance

We presented data from the first samples collected directly from discharge of a ridge-flank, cool hydrothermal system (CHS). We observed small but measurable differences in ion concentrations between Dorado Outcrop CHS fluids and bottom seawater (Table 1). Given the slow kinetics of inorganic reactions at low temperatures, much of the observed change in composition is likely to be aided by microbial catalyzed reactions. Whether such changes are from abiotic and/or biotic reactions, measured change, if representative of global conditions, significantly affect global oceanic budgets for Rb, Mo, V, U, Mg, phosphate, and Li. Given that these calculations result in significant geochemical fluxes, continued work with the CHS at Dorado Outcrop, and similar systems in other settings (yet to be discovered), is important for understanding global elemental budgets.

The presence of DO in CHS fluids (Fig. 3, Table 1) is a consequence of rapid lateral flow and slow reaction kinetics within the upper basaltic crust across tens of kilometers, and is consistent with oxic conditions in the upper basaltic crust more generally (D'Hondt et al., 2015). An oxic basaltic crustal fluid implies that aerobic microbial processes should dominate within hydrologic regions of the upper oceanic crust, potentially persisting in the upper crust for millions of years, as long as the crust remains permeable and hydrologically connected to the overlying ocean. Microorganisms involved in anaerobic metabolic pathways (e.g., methanogenesis, sulfate reduction, ammonia oxidation) may be found in spring fluids and on rock surfaces bathed in spring fluids, as they were on basaltic rocks collected from Dorado Outcrop (e.g., Lee et al., 2015). Such microorganisms could reside in either the overlying organic-rich sediment or in basaltic crust that is marginally affected by CHS, or in anaerobic microniche that form in reduced basaltic environments that are minimally connected to oxic hydrologic pathways (e.g., Rouxel et al., 2008; Alt and Shanks, 2011; Lever et al., 2013).

Dorado Outcrop is the first location where discharging CHS fluids have been discovered and sampled. This system is likely to be broadly representative in terms of the chemical composition of global CHS systems, even if the setting is somewhat unusual, because low temperature and short residence time in the crust are primary factors controlling the extent of water–rock interaction for these systems. Locating and sampling additional CHSs will improve understanding of the global influence of these ubiquitous systems. It will be particularly helpful to sample fluids that discharge from CHSs across a range of temperatures ($\leq$20 °C), to determine likely systematic variations in fluid composition with discharging temperature, such as those suggested for phosphate and Mg (Fisher and Wheat, 2010). This presents technical challenges, both to locate new CHS discharge sites and to collect pristine samples without entraining bottom water. Studies of these systems are also challenged by the accuracy of analytical techniques, because the compositional differences between CHS fluids and bottom seawater are small. Future studies should also account for hydrogeologic dynamics in flow rates, temperatures, and chemical compositions when developing a holistic understanding of CHS impacts.

Author contributions

C.G.W., A.T.F., and S.M.H. conceived and designed the experiment, secured ship time and oversaw submersible operations. All coauthors participated in sample collection, co-wrote the paper, and drafted the figures. C.G.W. and J.M. analyzed the spring fluids. A.T.F. interpreted seismic data and calculated upper basement temperatures. S.M.H. processed bathymetric data. B.N.O. measured dissolved oxygen in sediment pore waters.

Acknowledgements

The authors thank the entire shipboard parties of cruises AT26-09 and AT26-24 for their contributions at sea, including the crews and pilots of the AUV *Sentry*, ROV *Jason II*, and HOV *ALVIN*. In particular, we thank Heiner Villinger's leadership in the detection of water column thermal anomalies, Chris Trabaol for assistance with multibeam data processing, and Trevor Fournier for assistance with fluid-sampling device preparation. J. Kleusner reprocessed seismic reflection data shown in Fig. 2. Brian Glazer provided the wiring and Aanderra optode for use with *ALVIN*. This research was supported by National Science Foundation grants OCE-1130146 (CGW), OCE-1131210 and OCE-1260408 (ATF) and grant OIA-0939564 to the Center for Dark Energy Biosphere Investigations (C-DEBI) Science and Technology Center (all authors). C-DEBI supported the contributions of JM and BO. This is C-DEBI contribution number 377.

Appendix A. Supplementary material

Supplementary material related to this article can be found online at http://dx.doi.org/10.1016/j.epsl.2017.07.049.

References

Alt, J.C., Shanks, W.C., 2011. Microbial sulfate reduction and the sulfur budget for a complete section of altered oceanic basalts, IODP Hole 1256D (eastern Pacific). Earth Planet. Sci. Lett. 310 (1), 73–83.

Anderson, B.W., Gillis, K.M., Coogan, L.A., 2013. A hydrologic model for the uppermost oceanic crust constrained by temperature estimates from carbonate minerals. J. Geophys. Res. Solid Earth 118, 3917–3930. http://dx.doi.org/10.1002/jgrb.50325.

Armstrong, F.A.J., Stearns, C.R., Strickland, J.D.H., 1967. The measurement of upwelling and subsequent biological processes by means of the Technicon Auto-Analyzer and associated equipment. Deep-Sea Res. 14 (3), 381–389.

Atlas, E.L., Hager, S.W., Gordon, L.I., Park, P.K., 1971. A Practical Manual for Use of the Technicon Autoanalyzer in Seawater Nutrient Analyses; Revised. Technical Report 215. Oregon State University, Dept of Oceanography. Ref. No. 71–22. 48 pp.

Bach, W., Edwards, K.J., 2003. Iron and sulfide oxidation within the basaltic ocean crust: implications for chemolithoautotrophic microbial biomass production. Geochim. Cosmochim. Acta 67 (20), 3871–3887.

Bernhardt, H., Wilhelms, A., 1967. The continuous determination of low level iron,soluble phosphate and total phosphate with the AutoAnalyzer. In: Technicon Symp., 1967, vol. I, p. 386.

Caress, D.W. Thomas, H. Kirkwood, W.J. McEwen, R. Henthorn, R. Clague, E.A. Paull, C.K. Paduan, J. Maier, K.L., High-Resolution Multibeam, Sidescan, and Subbottom Surveys Using the MBARI AUV D. Allan B, in: Reynolds, J.R., Greene, H.G., (Eds.), Marine Habitat Mapping Technology for Alaska, Alaska Sea Grant College Program, University of Alaska Fairbanks, 2008. http://dx.doi.org/10.4027/mhmta.2008.04.

Coogan, L.A., Parrish, R.R., Roberts, N.M., 2016. Early hydrothermal carbon uptake by the upper oceanic crust: insight from in situ U–Pb dating. Geology 44 (2), 147–150.

Corliss, J.B., Dymond, J., Gordon, L.I., Edmond, J.M., von Herzen, R.P., Ballard, R.D., Green, K., Williams, D., Bainbridge, A., Crane, K., van Andel, t.H., 1979. Submarine thermal springs on the Galapagos Rift. Science 203, 1073–1083.

Davis, E.E., Chapman, D.S., Wang, K., Villinger, H., Fisher, A.T., Robinson, S.W., Grigel, J., Pribnow, D., Stein, J., Becker, K., 1999. Regional heat-flow variations across the sedimented Juan de Fuca ridge eastern flank: constraints on lithospheric cooling and lateral hydrothermal heat transport. J. Geophys. Res. 104 (B8), 17,675–17,688.

Davis, E.E., Chapman, D.S., Mottl, M.J., Bentkowski, W.J., Dadey, K., Forster, C., Harris, R., Nagihara, S., Rohr, K., Wheat, C.G., Whiticar, M., 1992. FlankFlux: an experiment to study the nature of hydrothermal circulation in young sea floor. Can. J. Earth Sci. 29, 925–952.

De Lange, G.J., Cranston, R.E., Hydes, D.H., Boust, D., 1992. Extraction of pore water from marine sediments: a review of possible artifacts with pertinent examples from the North Atlantic. Mar. Geol. 109, 53–76.

D'Hondt, S., Inagaki, F., Zarikian, C.A., Abrams, L.J., Dubois, N., Engelhardt, T., Evans, H., Ferdelman, T., Gribsholt, B., Harris, R.N., Hoppie, B.W., Hyun, J.-H., Kallmeyer, J., Kim, J., Lynch, J.E., McKinley, C.C., Mitsunobu, S., Morono, Y., Murray, R.W., Pockalny, R., Sauvage, J., Shimono, T., Shiraishi, F., Smith, D.C., Smith-Duque, C.E., Spivack, A.J., Steinsbu, B.O., Suzuki, Y., Szpak, M., Toffin, L., Uramoto, G., Yamaguchi, Y.T., Zhang, G., Zhang, X.-H., Ziebis, W., 2015. Presence of oxygen and

aerobic communities from sea floor to basement in deep-sea sediments. Nat. Geosci. online 16 March 2015.
Elderfield, H., Schultz, A., 1996. Mid-ocean ridge hydrothermal fluxes and the chemical composition of the ocean. Annu. Rev. Earth Planet. Sci. 24, 191–224.
Elderfield, H., Wheat, C.G., Mottl, M.J., Monnin, C., Spiro, B., 1999. Fluid and geochemical transport through oceanic crust: a transect across the eastern flank of the Juan de Fuca Ridge. Earth Planet. Sci. Lett. 172 (1), 151–165.
Feely, R.A., Trefry, J.H., Lebon, G.T., German, C.R., 1998. The relationship between P/Fe and V/Fe ratios in hydrothermal precipitates and dissolved phosphate in seawater. Geophys. Res. Lett. 25 (13), 2253–2256.
Fisher, A.T., Wheat, C.G., 2010. Seamounts as conduits for massive fluid, heat and solute fluxes on ridge flanks. Oceanography 23 (1), 74–87.
Fisher, A.T., Harris, R., 2010. Using seafloor heat flow as a tracer to map subseafloor fluid flow in the ocean crust. Geofluids. http://dx.doi.org/10.1111/j.1468-8123.2009.00274.x.
Fisher, A.T., Stein, C.A., Harris, R.N., Wang, K., Silver, E.A., Pfender, M., Hutnak, M., Cherkaoui, A., Bodzin, R., Villinger, H., 2003. Abrupt thermal transition reveals hydrothermal boundary and role of seamounts within the Cocos Plate. Geophys. Res. Lett. 30 (11), 1550. http://dx.doi.org/10.1029/2002GL016766.
Gordon, L.I., Jennings Jr., J.C., Ross, A.A., Krest, J.M., 1994. A Suggested Protocol for Continuous Flow Analysis of Seawater Nutrients (Phosphate, Nitrate, Nitrite, and Silicic Acid) in the WOCE Hydrographic Program and the Joint Global Ocean Fluxes Study. WHP Office Report 91-1. Revision 1.
Hart, S.R., Staudigel, H., 1982. The control of alkalies and uranium in seawater by ocean crust alteration. Earth Planet. Sci. Lett. 58 (2), 202–212.
Hulme, S., 2015. NOAA National Centers for Environmental Information (2004): Multibeam Bathymetry Database (MBBDB), [AT26-09-auv]. NOAA National Centers for Environmental Information. http://dx.doi.org/10.7289/V56T0JNC.
Hutnak, M., Fisher, A.T., Stein, C.A., Harris, R., Wang, K., Silver, E., Spinelli, G., Pfender, M., Villinger, H., MacKnight, R., Costa Pisani, P., DeShon, H., Diamente, C., 2007. The thermal state of 18–24 Ma upper lithosphere subducting below the Nicoya Peninsula, northern Costa Rica margin. In: Dixon, T., et al. (Eds.), MARGINS Theoretical Institute: SIEZE Volume. Columbia University Press, New York, pp. 86–122.
Hutnak, M., Fisher, A.T., Harris, R., Stein, C., Wang, K., Spinelli, G., Schindler, M., Villinger, H., Silver, E., 2008. Large heat and fluid fluxes driven through mid-plate outcrops on ocean crust. Nat. Geosci. http://dx.doi.org/10.1038/ngeo264.
Jannasch, H.W., Wheat, C.G., Plant, J., Kastner, M., Stakes, D., 2004. Continuous chemical monitoring with osmotically pumped water samplers: OsmoSampler design and applications. Limnol. Oceanogr., Methods 2, 102–113.
Johnson, H.P., Pruis, M.J., 2003. Fluxes of fluid and heat from the oceanic crustal reservoir. Earth Planet. Sci. Lett. 216 (4), 565–574.
Langseth, M.G. Hyndman, R.D. Becker, K. Hickman, S.H. Salisbury, M.H., 1984. The hydrogeological regime of isolated sediment ponds in mid-oceanic ridges. US Govt. Printing Office; UK distributors, IPOD Committee, NERC, Swindon.
Lee, M.D., Walworth, N.G., Sylvan, J.B., Edwards, K.J., Orcutt, B.N., 2015. Microbial communities on seafloor basalts at Dorado Outcrop reflect level of alteration and highlight global lithic clades. Front. Microbiol., 1–20. http://dx.doi.org/10.3389/fmicb.2015.01470. published 23 December 2015.
Lever, M.A., Rouxel, O., Alt, J.C., Shimizu, N., Ono, S., Coggon, R.M., Shanks, W.C., Lapham, L., Elvert, M., Prieto-Mollar, X., Hinrichs, K.U., 2013. Evidence for microbial carbon and sulfur cycling in deeply buried ridge flank basalt. Science 339 (6125), 1305–1308.
Lister, C.R.B., 1972. On the thermal balance of a mid-ocean ridge. Geophys. J. Int. 26 (5), 515–535.
Macdonald, K.C., Fox, P.J., Alexander, R.T., Pockalny, R., 1996. Volcanic growth faults and the origin of Pacific abyssal hills. Nature 380, 125–129.
McCue, S., Yoerger, D., 2010. Near-bottom multibeam surveys for deep sea scientific applications. In: Reson User Conference. St Petersburg, FL, Oct 2010. https://www.whoi.edu/fileserver.do?id=73430&pt=10&p=49058, 2010.
Mottl, M., 2003. Partitioning of energy and mass fluxes between mid-ocean ridge axes and flanks at high and low temperature. In: Halbach, P., Tunnicliffe, V., Hein, J. (Eds.), Energy and Mass Transfer in Submarine Hydrothermal Systems. Dahlem University Press, Berlin, Germany, pp. 271–286.
Mottl, M.J., Wheat, C.G., Baker, E., Becker, N., Davis, E., Feely, R., Grehan, A., Kadko, D., Lilley, M., Massoth, G., Moyer, C., Sansone, F., 1998. Warm springs discovered on 3.5 Ma-old oceanic crust, eastern flank of the Juan de Fuca Ridge. Geology 26, 51–54.
Orcutt, B.N., Wheat, C.G., Rouxel, O., Hulme, S., Edwards, K.J., Bach, W., 2013. Oxygen consumption rates in subseafloor basaltic crust derived from a reaction transport model. Nat. Commun., 1–8. http://dx.doi.org/10.1038/ncomms3539. published 27 Sep 2013.
Patton, C.J., 1983. Design, Characterization and Applications of a Miniature Continuous Flow Analysis System. Ph.D. Thesis, Mich. State U., U. Microfilms International, Ann Arbor, Mich. 150 pp.
Rouxel, O., Ono, S., Alt, J., Rumble, D., Ludden, J., 2008. Sulfur isotope evidence for microbial sulfate reduction in altered oceanic basalts at ODP Site 801. Earth Planet. Sci. Lett. 268 (1), 110–123.
Sclater, J.G., Jaupart, C., Galson, D., 1980. The heat flow through oceanic and continental crust and the heat loss of the Earth. Rev. Geophys. Space Phys. 18, 269–311.
Seyfried, W.E., 1977. Seawater–Basalt Interaction from 25°–300 °C and 1–500 Bars: Implications for the Origin of Submarine Metal-Bearing Hydrothermal Solutions and Regulation of Ocean Chemistry. Ph.D. dissertation, Univ. Southern California. 242 pp.
Spinelli, G.A., Underwood, M.B., 2004. Character of sediments entering the Costa Rica subduction zone: implications for partitioning of water along the plate interface. Isl. Arc 13 (3), 432–451.
Spinelli, G.A., Giambalvo, E.R., Fisher, A.T., 2004. Sediment permeability, distribution, and influence on fluxes in oceanic basement. In: Davis, E.E., Elderfield, H. (Eds.), Hydrogeology of the Oceanic Lithosphere. Cambridge University Press, Cambridge, UK.
Staudigel, H., Hart, S.R., Richardson, S.H., 1981. Alteration of oceanic crust: processes and timing. Earth Planet. Sci. Lett. 52, 311–327.
Stein, C., Stein, S., 1994. Constraints on hydrothermal heat flux through the oceanic lithosphere from global heat flow. J. Geophys. Res. 99, 3081–3095.
Wheat, C.G., Mottl, M.J., 2004. Geochemical fluxes through mid-ocean ridge flanks. In: Davis, E.E., Elderfield, H. (Eds.), Hydrogeology of the Oceanic Lithosphere. Cambridge University Press, Cambridge, UK, pp. 627–658.
Wheat, C.G., Fisher, A.T., 2007. Seawater recharge along an eastern bounding fault in Middle Valley, northern Juan de Fuca Ridge. Geophys. Res. Lett. 34, L20602. http://dx.doi.org/10.1029/2007GL031347.
Wheat, C.G., Fisher, A.T., 2008. Massive, low-temperature hydrothermal flow from a basaltic outcrop on 23 Ma seafloor of the Cocos Plate: chemical constraints and implications. Geochem. Geophys. Geosyst. 9, Q12O14. http://dx.doi.org/10.1029/2008GC002136.
Wheat, C.G., McManus, J., Mottl, M., Giambalvo, E.G., 2003. Oceanic phosphorus imbalance: magnitude of the mid-ocean ridge flank hydrothermal sink. Geophys. Res. Lett. 30. http://dx.doi.org/10.1029/2003GL017318.
Wheat, C.G., Mottl, M.J., Fisher, A.T., Kadko, D., Davis, E.E., Baker, E., 2004. Heat flow through a basaltic outcrop on a sedimented young ridge flank. Geochem. Geophys. Geosyst. 5, Q12006. http://dx.doi.org/10.1029/2004GC000700.
Wheat, C.G., Jannasch, H.W., Kastner, M., Hulme, S., Cowen, J., Edwards, K., Orcutt, B.N., Glazer, B., 2011. Fluid sampling from oceanic borehole observatories: design and methods for CORK activities (1990–2010). In: Fisher, A.T., Tsuji, T., Petronotis, K., the Expedition 327 Scientists (Eds.), Proc. IODP, vol. 327. Integrated Ocean Drilling Program Management International, Inc., Tokyo.
Winslow, D.M., Fisher, A.T., 2015. Sustainability and dynamics of outcrop-to-outcrop hydrothermal circulation. Nat. Commun. http://dx.doi.org/10.1038/ncomms8567.
Winslow, D.M., Fisher, A.T., Stauffer, P.H., Gable, C.W., Zyvoloski, G.A., 2016. Three-dimensional modeling of outcrop-to-outcrop hydrothermal circulation on the eastern flank of the Juan de Fuca Ridge. J. Geophys. Res., Solid Earth 121. http://dx.doi.org/10.1002/2015JB012606.
Ziebis, W., McManus, J., Ferdelman, T., Schmidt-Schierhorn, F., Bach, W., Muratli, J., Edwards, K.J., Villinger, H., 2012. Interstitial fluid chemistry of sediments underlying the North Atlantic gyre and the influence of subsurface fluid flow. Earth Planet. Sci. Lett. 323, 79–91.